A ϕ-Model Solution for the Inverse Position Problem of Calibrated Robots Using Virtual Elementary Motions.

Ibrahim A. Sultan
School of Engineering
University of Ballarat
PO Box 663
Ballarat VIC 3350
Australia

John G. Wager
Department of Mechanical and Materials Engineering
The University of Western Australia
Nedlands WA 6907
Australia

Keywords: Robots – Kinematic Modelling – Position Analysis – Transformation.

Abstract:

It is central to the control of manipulators to calculate the set/sets of joint-displacements which correspond to a given spatial pose (position and orientation) of the end-effector. This problem, which is referred to as the inverse position problem, represents one of the most difficult mathematical challenges in the field of robotics, particularly when performed for calibrated robots (or robots with general structures). In such cases, closed form solutions are too impractical to implement and iterative solutions suffer from numerical singularities.

In the present work a procedure is introduced to obtain multiple inverse position solutions for serial robotic structures. For calibrated robots, the procedure involves a simple iterative technique designed to ensure fast convergence and eliminate the occurrence of singularity. However, inverse position solutions for spherical-wrist manipulators will be obtained in a straight-forward non-iterative fashion. A published kinematic notation, referred to as the ϕ-model, was used to develop the system equations.

1. Introduction and Problem Statement:

The main function of a robot manipulator in industrial applications is to place an object (tool or end-effector) at a given spatial pose (position and orientation). Since any unconstrained such pose is defined by six independent parameters, three for position and three for orientation, the robot may have to possess at least six degrees of freedom to be dextrous enough for flexible automation and other applications. Therefore robots are often provided with six single-degree-of-freedom joints of a rotary or sliding type. These particular kinematic pairs are used due to the ease they provide for powering and control.

Position (or kinematic) analysis of robotic manipulators is often performed by attaching a set of Cartesian frames to the successive links on the structure and constructing a corresponding set of 4x4 matrices (Homogeneous Transformation matrices) to perform transformation between these frames. Usually the Z-axes of the link frames coincide with the axes of the manipulator joints. The Homogeneous Transformation matrix, ${}_{i}\mathbf{T}^{i+1,}$ uses a set of geometric parameters to express the spatial particulars of Cartesian frame number i+1 with respect to frame number i. These parameters (4 or 5 depending on the

model used) may be divided into link parameters and joint parameters. While the link parameters reflect on the geometric features of the manipulator link (length, twist, …etc), a joint parameter indicates the amount of displacement (angular or linear) performed by the joint connecting the two successive frames. The spatial particulars of frame number *n* (which is always attached to the tool) with respect to the base frame, number 0, can be obtained by a matrix chain product as follows;

$$ {}_0\mathbf{T}^{\mathbf{n}} = {}_0\mathbf{T}^1 \, {}_1\mathbf{T}^2 \, {}_2\mathbf{T}^3 \cdots {}_{\mathbf{n}-2}\mathbf{T}^{\mathbf{n}-1} \, {}_{\mathbf{n}-1}\mathbf{T}^{\mathbf{n}} \qquad (1) $$

If the set of joint displacements are known, i.e. all the matrices ${}_i\mathbf{T}^{i+1}$ are given, equation (1) may be used to calculate the matrix, ${}_0\mathbf{T}^{\mathbf{n}}$. Such straightforward procedure is always referred to as the *direct position analysis*. On the other hand, the *inverse position analysis* is performed to calculate the set (or sets) of joint displacements which correspond to a known spatial particulars of the end-effector frame, i.e. ${}_0\mathbf{T}^{\mathbf{n}}$ is given and all the transformation matrices, ${}_i\mathbf{T}^{i+1}$ should be worked out. This problem represents a special difficulty in the field of robot control and a good deal of literature was published to deal with it. Examples of the published literature are reviewed in the next section.

2. Literature Survey:

Published literature reveals that the homogeneous transformation matrix which was developed by Denavit and Hartenberg (1955) has extensively been employed for the analysis of robot manipulators. The matrix involves the use of four parameters, usually referred to as the DH-parameters, intended to perform transformation between two spatial Cartesian coordinate systems. Sultan and Wager (1999) reflect on the aspects of the

models used to describe the kinematic behaviour of manipulators. They then propose a zero-initial position notation (referred to as the ϕ-model) which has been designed to be complete and non-singular. This is particularly important if the model is going to be implemented for robot calibration purposes. Pennock and Yang (1985), Gu and Luh (1987) and Pardeep *et al* (1989) reported techniques which utilise the theory of dual-number algebra as presented to the field of kinematics by Yang and Freudenstein (1964). In addition to these approaches, which are based on matrices, vector methods were also employed in the field of kinematic analysis of robots by Duffy (1980) and Lee and Liang (1988A & 1988B.)

Many industrial robots possess parallel and intersecting joint-axes and their direct-position models can be inverted analytically such that closed-form solutions may be obtained for the joint-displacements. Examples of such approaches have been published by Gupta (1984), Pennock and Yang (1985), Pardeep *et al* (1989), Wang and Bjorke (1989) and other researchers.

Spherical-wrist manipulators have their last three joint-axes intersecting at a common point. For these manipulators the position of the end-effector in space is determined only by the displacements performed about the first three joint-axes. This concept is often referred to as the position-orientation decoupling and was first utilised by Pieper and Roth (1969) to produce a closed form solution, for the inverse position problem of simple structure robots, efficient enough to be implemented for computer control. Sultan and Trevelyan (1992) also utilise the decoupling theory but their approach does not require

any particular spatial relations (e.g. parallelism or perpendicularity) between the arm joint-axes. However all approaches which utilise particular geometric features (such as the spherical-wrist property) of the manipulator structures are likely to produce positioning errors since the actual structures always deviate from their intended geometry.

Iterative techniques have been employed by researchers for the inverse position analysis of general robot manipulators. Many of these techniques involve the computation of a Jacobian matrix which has to be calculated and inverted at every iteration. The solution in this case may be obtained by a Newton-Raphson technique as reported by Hayati and Reston (1986) or a Kalman filter approach in a manner similar to that described by Coelho and Nunes (1986). The inversion of the system Jacobian may not be possible near singular configurations (where the motion performed about one joint-axis produces exactly the same effect, at the end-effector, as the motion performed about another axis, hence resulting in loss of one or more degrees of freedom). Therefore, Chiaverini *et al* (1994) report a singularity avoidance approach where the technique of damped least-squares is used for the analysis. However, this technique seems to be rather sluggish near singular points and extra computational procedure may have to be involved.

Optimisation techniques are also employed to solve the inverse-position problem of manipulators as reported by Goldenberg *et al* (1985) who implemented a six-element error vector for the analysis. The vector combines the current spatial information (position and orientation) of the robot hand and compares it to the desired pose to

produce error values. Fast-converging numerical procedure is then proposed and implemented to calculate the set of joint-displacements that minimises the error quantities. The procedure can be used for both redundant and non-redundant manipulators and is able to account for the physical displacement limits of the various joints. The work also offers valuable insights into such issues as step size control and the formulation of the Jacobian matrix. It was found that the convergence would improve considerably if the Jacobian was analytically determined. Other optimisation techniques have been published by Mahalingam and Sharan (1987) and Wang and Chen (1991) who employed a technique by which the robot is moved about one joint at a time to close an error gap. Techniques developed about this idea were also reported by Sultan *et al* (1987) and Poon and Lawrence (1988).

Manseur and Doty (1992A & 1992B) and (1996) described the kinematic behaviour of robots in terms of simplified polynomials that can be solved iteratively. A similar approach was adopted by Tsai and Morgan (1985) who described the kinematic behaviour of robots in terms of eight polynomials which were then solved numerically to obtain different possible solutions to the inverse position problem. They arrived at the conclusion that the maximum number of meaningful solutions to the inverse position problem of a general robotic structure is 16 not 32 as was suggested by Duffy and Crane (1980). However Manseur and Doty (1989) point out that a manipulator with 16 different real inverse position solutions can seldom be found in real life. In reality most manipulators are designed to possess up to 8 solutions of which only one or two can be physically attained.

Lee and Liang (1988A & 1988B) express the inverse position problem of robots in terms of a 16 degree polynomial in the tan-half-angle of a joint-displacement. A similar polynomial was developed by Raghavan and Roth (1989). However Smith and Lipkin (1990) argue that the coefficients of such polynomials are likely to contain too many terms which may render them impractical to use. Also, these polynomials are obtained by evaluating the eliminants of hyper-intricate determinants which may be impossible to handle symbolically in the first place. This may have motivated Manocha and Canny (1992) and Kohli and Osvatic (1993) to reformulate the solutions in form of elegant eigenvalue models in order to simplify the analysis and avoid numerical complications.

The procedure proposed here for the inverse position analysis of robot manipulators is described in the rest of this paper.

3. Kinematic Notation:

The work presented in this paper has been developed using a published kinematic notation referred to as the ϕ-model, Sultan and Wager (1999). The notation possesses the property of zero-initial-position. By virtue of this property the robot can be set at any desired home position where all the joint-displacements are conveniently assigned the value of zero. This section is not intended to offer a full discussion on the characteristics of the notation, since this may be sought in the publication indicated above, but rather to briefly review the portion of its mathematical framework which is relevant to the content of this paper.

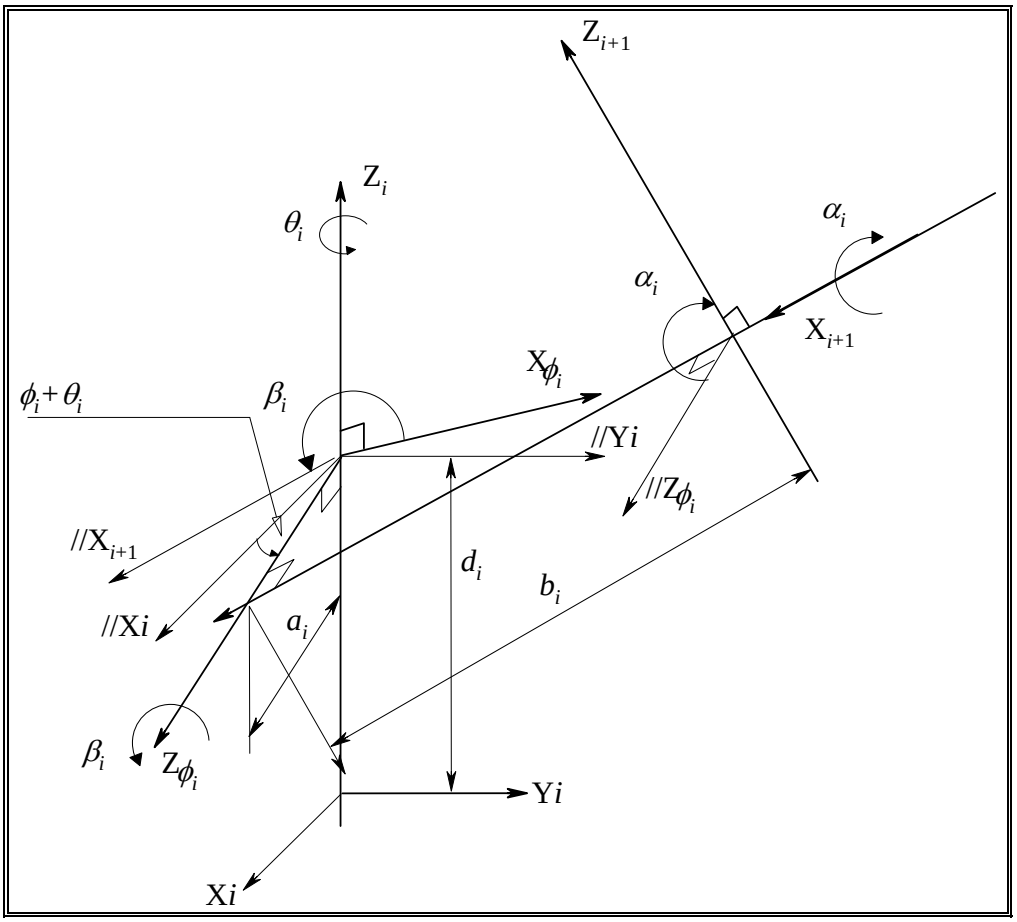

Figure (1): The Kinematic Notation of the ϕ-Model.

The kinematic aspects of the ϕ-model notation are shown in Figure (1). The model is established by introducing an intermediate Cartesian system between the joint-frames number (*i)* and (*i*+1). The Z-axis of the new frame, which is referred to as the ϕ_i-frame, lies in a plane parallel to the X_iY_i-plane and at a distance, d_i, equal to the linear joint-displacement from it. In case of a rotary joint, d_i may be set equal to zero. This Z-axis, which may be referred to as $Z_{\phi i}$, is initially set by the user at a constant angle, ϕ_i, from

the X_i-axis. ϕ_i, which is measured in a right-handed sense about Z_i, is selected to ensure that $Z_{\phi i}$ may not be parallel to Z_{i+1}. The $X_{\phi i}$-axis of the ϕ_i-frame is then established in a plane perpendicular to both $Z_{\phi i}$ and Z_i. The ϕ_i-frame is then used to establish a Cartesian system, $X_{i+1}Y_{i+1}Z_{i+1}$, about the Z_{i+1}-axis in a DH-fashion. The ϕ_i-frame and the (i+1)-frame are on the same rigid link and perform the same displacement (d_i or θ_i) along or about the Z_i respectively.

The transformation, ${}_i\mathbf{T}^{i+1}$, relating the (i+1)-frame to the i-frame may now be expressed as follows,

$$ {}_i\mathbf{T}^{i+1} = {}_i\mathbf{T}^{\phi_i}\ {}_{\phi i}\mathbf{T}^{i+1} \tag{2} $$

where ${}_i\mathbf{T}^{\phi_i}$ and ${}_{\phi i}\mathbf{T}^{i+1}$ represent the transformation relating the ϕ_i-frame to the i-frame and the (i+1)-frame to the ϕ_i-frame respectively. These matrices may be expressed as follows,

$$ {}_i\mathbf{T}^{\phi_i} = \begin{bmatrix} -\sin(\phi_i + \theta_i) & 0 & \cos(\phi_i + \theta_i) & 0 \\ \cos(\phi_i + \theta_i) & 0 & \sin(\phi_i + \theta_i) & 0 \\ 0 & 1 & 0 & d_i \\ 0 & 0 & 0 & 1 \end{bmatrix} $$

and (3)

$$ {}_{\phi_i}\mathbf{T}^{i+1} = \begin{bmatrix} \cos(\beta_i) & -\sin(\beta_i)\cos(\alpha_i) & \sin(\beta_i)\sin(\alpha_i) & b_i\cos(\beta_i) \\ \sin(\beta_i) & \cos(\beta_i)\cos(\alpha_i) & -\cos(\beta_i)\sin(\alpha_i) & b_i\sin(\beta_i) \\ 0 & \sin(\alpha_i) & \cos(\alpha_i) & a_i \\ 0 & 0 & 0 & 1 \end{bmatrix} $$

where a_i, b_i, α_i and β_i are the DH-parameters which relate the (i+1)-frame to the ϕ_i-frame as shown in Figure (1). As the above expression for ${}_i\mathbf{T}^{\phi_i}$ indicates, the angle between the X_i- and the $Z_{\phi i}$-axes is initially ϕ_i. However with the onset of the rotational motion, this angle would vary by the value of the motor displacement, θ_i. The expression also reveals that the ϕ_i-frame may slide along the Z_i-axis a distance d_i if the joint was of the sliding type; in such a case θ_i may be set equal to zero.

To render the model complete such that arbitrarily-located frames (e.g. the tool frame, which may be predetermined by the requirements of some manufacturing set-up rather than assigned systematically according to the rules of the ϕ-model, or any other model for this matter) can be described, a rotation, γ_i, and a translation, h_i, may be performed about and along the Z_{i+1}-axis. The new $(i+1)$-frame can now be related to the ϕ_i-frame by the following equation,

$$ {}_{\phi i}\mathbf{T}^{i+1} = \text{Trans}(0, 0, a_i)\ \text{Rot}(\mathbf{z}, \beta_i)\ \text{Trans}(b_i, 0, 0)\ \text{Rot}(\mathbf{x}, \alpha_i)\ \text{Rot}(\mathbf{z}, \gamma_i)\ \text{Trans}(0, 0, h_i) \tag{4} $$

In a more expanded form equation (4) can be re-expressed as follow;

$$ {}_{\phi_i}\mathbf{T}^{i+1} = \begin{bmatrix} \cos(\beta_i) & -\sin(\beta_i)\cos(\alpha_i) & \sin(\beta_i)\sin(\alpha_i) & b_i\cos(\beta_i) \\ \sin(\beta_i) & \cos(\beta_i)\cos(\alpha_i) & -\cos(\beta_i)\sin(\alpha_i) & b_i\sin(\beta_i) \\ 0 & \sin(\alpha_i) & \cos(\alpha_i) & a_i \\ 0 & 0 & 0 & 1 \end{bmatrix} \begin{bmatrix} \cos(\gamma_i) & -\sin(\gamma_i) & 0 & 0 \\ \sin(\gamma_i) & \sin(\gamma_i) & 0 & 0 \\ 0 & 0 & 1 & h_i \\ 0 & 0 & 0 & 1 \end{bmatrix} \tag{5} $$

4. Model Reduction:

The inverse-position model of any 6-degree-of-freedom serial-manipulator can be reduced to a 5-degree-of-freedom-model where the position of the last joint may be dealt with separately. This reduction will result in a simpler model where the manipulator may be regarded as a 5-degree-of-freedom serial mechanism attempting to locate the axis of the sixth joint at a desired pose (location and direction) in space.

Usually the end-effector frame, $X_eY_eZ_e$, is related to a Cartesian frame attached to joint-axis number 6, $X_6Y_6Z_6$, by a homogeneous transformation matrix, ${}_6\mathbf{T}^e$. This matrix may be expressed in terms of any convenient kinematic representation. If the ϕ-model was used for that purpose, the matrix ${}_6\mathbf{T}^e$ may be calculated as follows,

$${}_6\mathbf{T}^e = {}_6\mathbf{T}^{\phi 6}\,{}_{\phi 6}\mathbf{T}^e \qquad (6)$$

where the matrix ${}_6\mathbf{T}^{\phi 6}$ is established as detailed in section (3) and ${}_{\phi 6}\mathbf{T}^e$ is constructed, as described in equation (5), to define the arbitrary location of the tool frame with respect to the coordinate system of the sixth joint, $X_6Y_6Z_6$.

Typically, the Z-axis of the $X_6Y_6Z_6$-frame is directed along the axis of the sixth joint and the spatial particulars of the tool frame with respect to the base coordinate system are given in form of a known homogeneous transformation matrix, ${}_0\mathbf{T}^e$. The sixth joint frame may be evaluated with respect to the base frame, ${}_0\mathbf{T}^6$, as follows,

$${}_0\mathbf{T}^6 = {}_0\mathbf{T}^e\,({}_6\mathbf{T}^e)^{-1} \qquad (7)$$

where the elements of the third and fourth columns of the matrix $({}_6\mathbf{T}^e)^{-1}$ do not include any reference to the variable joint-displacement, θ_6. This may be attributed to the fact that the elements of these third and fourth columns respectively represent the unit vector of the sixth joint-axis and the position vector of the origin of the sixth joint-frame with respect to the tool frame. Both vectors are not affected by rotations performed about the sixth joint-axis and are respectively given as follows,

$$\begin{bmatrix} \sin(\beta_6)\cos(\gamma_6)+\cos(\beta_6)\cos(\alpha_6)\sin(\gamma_6) \\ -\sin(\beta_6)\sin(\gamma_6)+\cos(\beta_6)\cos(\alpha_6)\cos(\gamma_6) \\ -\cos(\beta_6)\sin(\alpha_6) \\ 0 \end{bmatrix} \text{ and } \begin{bmatrix} -b_6\cos(\gamma_6)-a_6\sin(\gamma_6)\sin(\alpha_6) \\ -a_6\cos(\gamma_6)\sin(\alpha_6)+b_6\sin(\gamma_6) \\ -h_6-a_6\cos(\gamma_6) \\ 1 \end{bmatrix}$$

where all parameters are as introduced in section (3).

Since these two columns will , after performing the matrix multiplication as per equation (7), produce the direction and position respectively of the sixth joint-axis with respect to the base frame, it may be concluded that the final pose of the sixth joint-axis is always fully defined in space at the outset of the inverse-position analysis. Since this axis is positioned in space solely by virtue of the motions performed by the first five joints on the manipulator structure next to the stationary base, the inverse position problem is reduced to finding the sets of five joint-displacements which correspond to a given spatial particulars of the sixth joint-axis on the manipulator.

In the following sections the models proposed for the solution of the inverse-position problem for robots are presented. In producing these models the 5R-manipulator has been regarded as consisting of two groups of joints where each group is assigned a

distinctive positioning task. The first group, which is referred to as the arm, consists of the first three joints on the manipulator structure next to the base. In the current context, the arm is assigned the task of positioning a given point on the sixth-joint axis at a required location in space.

The second joint group, which is referred to as the wrist, consists of the fourth and fifth joints on the manipulator structure. This group is assigned the task of aligning the sixth joint-axis with a given spatial orientation.

In calibrated robots where the property of spherical wrist is no longer realised, positioning tasks may not be distinctively distinguished but the two joint groups will collaborate to position the sixth joint-axis in the required pose. This characteristic has been utilised below to produce an approach for inverse position analysis of calibrated robots.

5. Positioning of the Arm:

A schematic diagram of an arm-group is shown in Figure (2). The arm, as depicted in this figure, consists of three rotary joints whose axes , Z_1, Z_2 and Z_3 are fully-defined in space with respect to a base coordinate system $X_0Y_0Z_0$. The initial location of the point, p^i, is given with respect to the base coordinates in terms of the position vector, $\mathbf{p}_0^i$. This point is required to be displaced to a new location, p^n, defined by the position vector $\mathbf{p}_0^n$ which is also given in terms of the base frame.

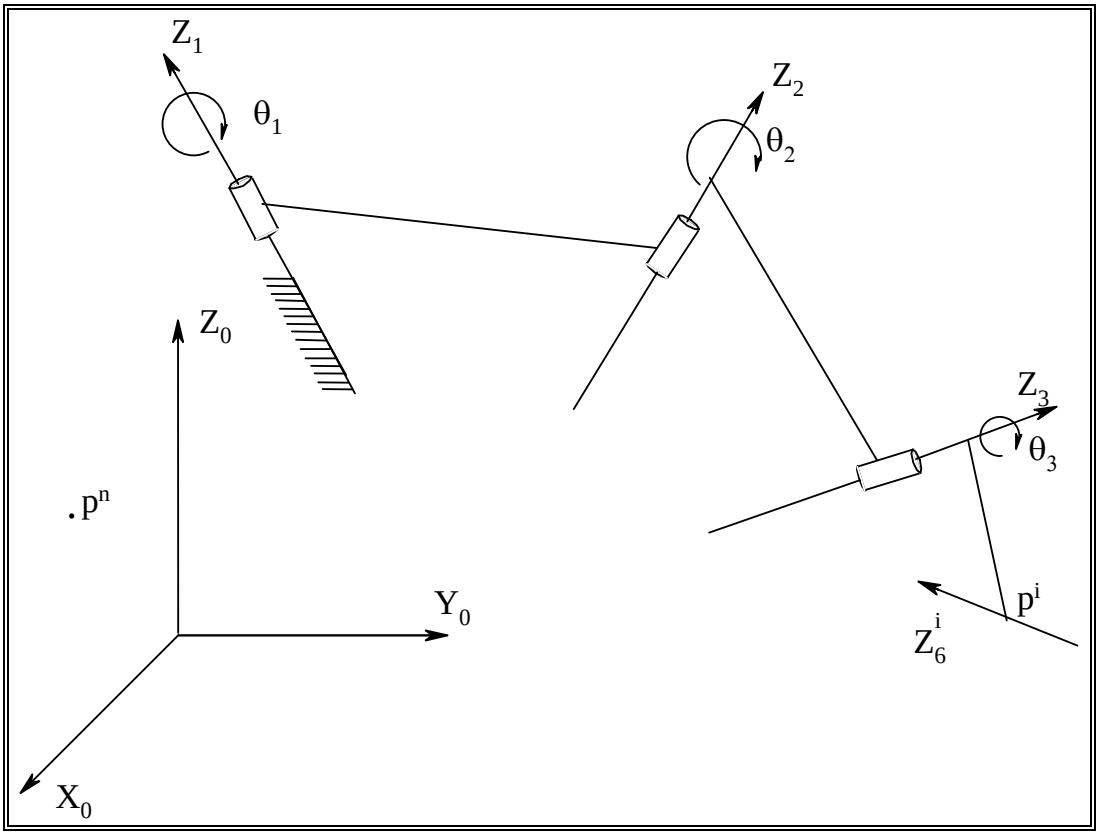

Figure (2): The Arm Positioning Group.

The location of point p^i with respect to a frame established about the axis $Z_{\phi 3}$ may be expressed in terms of the position vector, $\mathbf{p}_{\phi 3}$ which is independent of the joint-displacements or arm configuration. This position vector can be calculated as follows,

$$\begin{bmatrix} \mathbf{p}_{\phi 3} \\ 1 \end{bmatrix} = {}_{\phi 3}\mathbf{T}^0 \begin{bmatrix} \mathbf{p}_0^i \\ 1 \end{bmatrix} \tag{8}$$

where ${}_{\phi 3}\mathbf{T}^0$ is the matrix which performs transformation relating the base frame to $Z_{\phi 3}$–frame at zero initial position of the manipulator. This matrix may be calculated as follows,

$${}_{\phi 3}\mathbf{T}^0 = \left({}_3\mathbf{T}^{\phi 3}\right)^{-1}\left({}_{\phi 2}\mathbf{T}^3\right)^{-1}\left({}_2\mathbf{T}^{\phi 2}\right)^{-1}\left({}_{\phi 1}\mathbf{T}^2\right)^{-1}\left({}_1\mathbf{T}^{\phi 1}\right)^{-1}\left({}_{\phi 0}\mathbf{T}^1\right)^{-1}\left({}_0\mathbf{T}^{\phi 0}\right)^{-1} \tag{9}$$

where all matrices are established as pointed out in section (3).

Since the matrix ${}_{\phi 3}\mathbf{T}^{0}$ is worked out at zero initial position, all joint-displacements in equation (9) will be assigned the value of zero.

The configuration of the arm will then change in a sense that causes point p^{i} to coincide with the required position p^{n}. The joint-displacements, θ_1, θ_2 and θ_3, which correspond to the new arm configurations are required. At the new configuration, the known position vector $\mathbf{p}_0^{\mathrm{n}}$ can be related to $\mathbf{p}_{\phi 3}$ as follows,

$$\left({}_1\mathbf{T}^{\phi 1}\right)^{-1}\left({}_{\phi 0}\mathbf{T}^{1}\right)^{-1}\left({}_0\mathbf{T}^{\phi 0}\right)^{-1}\begin{bmatrix}\mathbf{p}_0^{\mathrm{n}}\\ 1\end{bmatrix}={}_{\phi 1}\mathbf{T}^{2}\,{}_2\mathbf{T}^{\phi 2}\,{}_{\phi 2}\mathbf{T}^{3}\,{}_3\mathbf{T}^{\phi 3}\begin{bmatrix}\mathbf{p}_{\phi 3}\\ 1\end{bmatrix} \tag{10}$$

where the matrices, ${}_1\mathbf{T}^{\phi 1}$, ${}_2\mathbf{T}^{\phi 2}$ and ${}_3\mathbf{T}^{\phi 3}$,contain reference to their corresponding joint-displacements as described in section (3).

The resulting vector quantities on the right- and left-hand sides of the equation (10) will be referred to below as $\mathbf{p}_R$ and $\mathbf{p}_L$ respectively. The following set of equations may then be written,

$$\mathbf{p}_{Lx} = \mathbf{p}_{Rx} \tag{11}$$

$$\mathbf{p}_{Lz} = \mathbf{p}_{Rz} \tag{12}$$

$$\mathbf{p}_{Ly} = \mathbf{p}_{Ry} \tag{13}$$

and

$$\mathbf{p}_L \circ \mathbf{p}_L = \mathbf{p}_R \circ \mathbf{p}_R \tag{14}$$

where ($\mathbf{p}_{Lx}$, $\mathbf{p}_{Ly}$ and $\mathbf{p}_{Lz}$) and ($\mathbf{p}_{Rx}$, $\mathbf{p}_{Ry}$ and $\mathbf{p}_{Rz}$) are the components of $\mathbf{p}_L$ and $\mathbf{p}_R$ respectively in the direction of the corresponding axes of the $X_{\phi_1}Y_{\phi_1}Z_{\phi_1}$-frame.

Generally, the above four equations contain linear combinations of S_1 and C_1 on their left-hand sides and non-linear combinations of S_2, C_2, S_3 and C_3 on their right-hand sides, where S_i refers to $sin(\theta_i)$ and C_i designates $cos(\theta_i)$. However the last two equations, (13) and (14), do not contain S_1 and C_1 by virtue of the kinematic aspects of rotation. When solved together these two equations will produce the following,

$$S_3 = \frac{f_1(S_2, C_2)}{f_2(S_2, C_2)}$$

and (15)

$$C_3 = \frac{f_3(S_2, C_2)}{f_2(S_2, C_2)}$$

where $f_1(S_2, C_2)$, $f_2(S_2, C_2)$ and $f_3(S_2, C_2)$ designate linear functions of S_2 and C_2.

Equations (15) may be combined with the well-known trigonometric identity ($S_3^2 + C_3^2 = 1$) to produce the following expression,

$$f_1^2(S_2, C_2) + f_3^2(S_2, C_2) = f_2^2(S_2, C_2) \quad (16)$$

where equation (16) is a second degree polynomial of S_2 and C_2.

Both S_2 and C_2 may be substituted for in equation (16) by the following trigonometric identities,

$$S_2 = \frac{-2t}{1+t^2}$$

and (17)

$$C_2 = \frac{1-t^2}{1+t^2}$$

where t refers to $tan(\frac{1}{2}\theta_2)$.

After due substitution equation (16) becomes a fourth-degree polynomial of t taking the following form,

$$\sum_{j=0}^{4} P_j t^j = 0 \quad (18)$$

where the values of the coefficient P_j depend on the arm dimensions and the initial and final locations of the positioned point. In the present work, a computer algebra package has been used to evaluate symbolic expressions for these coefficients.

It may be concluded from equation (18) that the inverse position problem of the arm possesses four possible solutions, where each solution corresponds to a distinctive configuration. For every solution, the corresponding root of t can be substituted in equations (17) to obtain unique values for S_2 and C_2. These values will be subsequently substituted in equations (15) such that both S_3 and C_3 may be uniquely calculated.

The analysis will be completed when the obtained values for S_2, C_2, S_3 and C_3 are eventually substituted in equations (11) and (12) to evaluate corresponding values for S_1

and C_1. Once all the sine- and cosine-terms have been found out, the *atan2* function is then implemented to calculate the corresponding angles.

The model proposed for the wrist joint group is presented in the next section.

6. Positioning of the Wrist:

The wrist consists of the fourth and fifth joints of the manipulator structure. In the present analysis, the joints of this group are assumed to stay locked until the arm joints have positioned a point defined on the sixth axis at a required location in space as described in section (5). Naturally, this will also displace the wrist joint-axes together with the sixth joint-axis to new spatial poses. At these poses the wrist joints are required to perform displacements in such a fashion that will align the sixth joint-axis with a desired spatial direction.

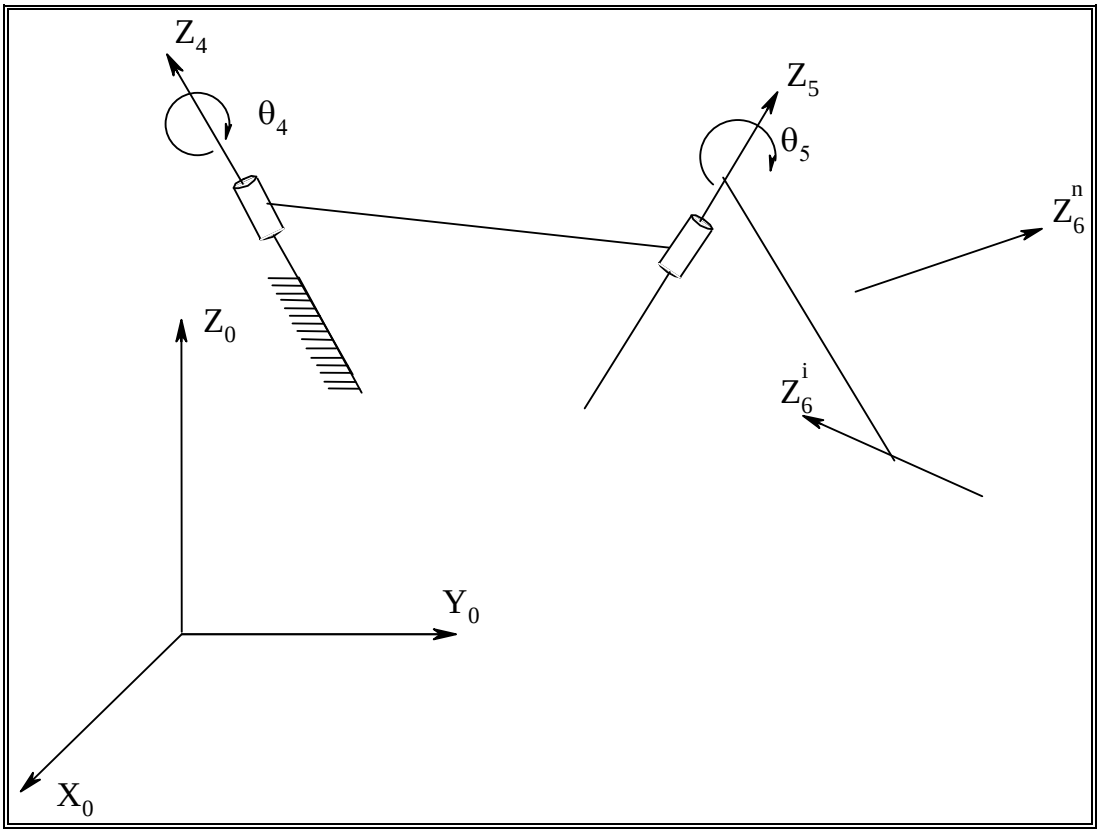

Figure (3): The Wrist Positioning Group.

A schematic diagram of the wrist joint-axes, Z_4 and Z_5, is shown in Figure (3). As depicted in this figure the direction of the axis Z_6^i is given with respect to the base-frame by the unit vector $\mathbf{z}_6^i$. This axis is required to be aligned with the axis Z_6^n whose direction, $\mathbf{z}_6^n$, is also given with respect to the same frame and the corresponding joint-displacements, θ_4 and θ_5, are to be obtained.

The direction of the axis Z_6^i may be expressed with respect to $X_{\phi_5}Y_{\phi_5}Z_{\phi_5}$-frame in terms of the constant unit vector $\mathbf{v}_{\phi 5}$ as follows,

$$\mathbf{v}_{\phi 5} = \left({}_{5}\mathbf{T}^{\phi 5}\right)^{-1}\left({}_{\phi 4}\mathbf{T}^{5}\right)^{-1}\left({}_{4}\mathbf{T}^{\phi 4}\right)^{-1}\left({}_{\phi 0}\mathbf{T}^{4}\right)^{-1}\left({}_{0}\mathbf{T}^{\phi 0}\right)^{-1}\mathbf{z}_{6}^{i} \tag{19}$$

where all **T**-matrices are established as described in section (3).

In equation (19), all joint-displacements may be assigned the value of zero because the directional vector, $\mathbf{v}_{\phi 5}$, is a constant that depends neither on the values of joint-displacements nor on the instantaneous configuration of the wrist.

The wrist joints may now perform displacements in a manner that would cause $\mathbf{z}_6^{\mathrm{i}}$ to take a direction parallel to that of $\mathbf{z}_6^{\mathrm{n}}$. At this new configuration $\mathbf{v}_{\phi 5}$ may be related to $\mathbf{z}_6^{\mathrm{n}}$ as follows,

$$\left({}_{4}\mathbf{T}^{\phi 4}\right)^{-1}\left({}_{\phi 0}\mathbf{T}^{4}\right)^{-1}\left({}_{0}\mathbf{T}^{\phi 0}\right)^{-1}\mathbf{z}_{6}^{n} = {}_{\phi 4}\mathbf{T}^{5}\,{}_{5}\mathbf{T}^{\phi 5}\mathbf{v}_{\phi 5} \tag{20}$$

where the matrices, ${}_{4}\mathbf{T}^{\phi 4}$ and ${}_{5}\mathbf{T}^{\phi 5}$, contain reference to their corresponding joint-displacements as described in section (3).

The vector quantities resulting on the right- and left-hand sides of the equation (20) will be referred to below as $\mathbf{z}_R$ and $\mathbf{z}_L$ respectively. The following set of equations may then be written,

$$\mathbf{z}_{Lx} = \mathbf{z}_{Rx} \tag{21}$$

$$\mathbf{z}_{Lz} = \mathbf{z}_{Rz} \tag{22}$$

and

$$\mathbf{z}_{Ly} = \mathbf{z}_{Ry} \tag{23}$$

where ($\mathbf{z}_{Lx}$, $\mathbf{z}_{Ly}$ and $\mathbf{z}_{Lz}$) and ($\mathbf{z}_{Rx}$, $\mathbf{z}_{Ry}$ and $\mathbf{z}_{Rz}$) are the components of $\mathbf{z}_L$ and $\mathbf{z}_R$ respectively in the direction of the corresponding axes of the $X_{\phi_4}Y_{\phi_4}Z_{\phi_4}$-frame.

Close investigation of equations (21) and (22) reveals that their left-hand sides and right-hand sides contain linear combinations of (S_4 and C_4) and (S_5 and C_5) respectively, where S_i refers to $sin(\theta_i)$ and C_i designates $cos(\theta_i)$. Equation (23) is a linear polynomial of S_5 and C_5 which may be substituted by the following trigonometric identities,

$$S_5 = \frac{-2t}{1+t^2} \quad \text{and} \quad C_5 = \frac{1-t^2}{1+t^2} \tag{24}$$

where t designates $tan(\frac{1}{2}\theta_5)$.

After due substitution equation (23) becomes a second degree polynomial of t as follows,

$$\sum_{j=0}^{2} P_j t^j = 0 \tag{25}$$

where the values of the coefficient P_j depend on the wrist dimensions and the initial and final orientations of the aligned axis.

Each root obtained for t, using equation (25), may be substituted in equations (24) to calculate the unique corresponding values of S_5 and C_5 which will be subsequently substituted in equations (21) and (22) to obtain the corresponding values for S_4 and C_4.

As revealed by equation (25), the inverse position analysis of the wrist group produces two distinctive solutions. In other words, this group possesses two configurations for each required orientation of the aligned axis.

7. The Inverse Solution Procedure:

Figure (4) depicts a flow chart that has been designed to explain the procedure proposed here for inverse position analysis of manipulators. As shown in the figure, the procedure features a simple iterative approach which does not involve any Jacobian matrix computations. Moreover, it produces multiple solutions to the problem which is a considerable advantage over other iterative methods. By virtue of the concepts presented, the various solutions may be calculated simultaneously if parallel computing facilities are available.

In the present approach, the arm is assigned the task of positioning any point on the sixth joint-axis at its required spatial location. The closest point on the sixth-joint axis to the fifth joint-axis may be conveniently selected for this purpose. This point will be referred to in the following discussion as p_0^i. The four joint-displacement solutions which

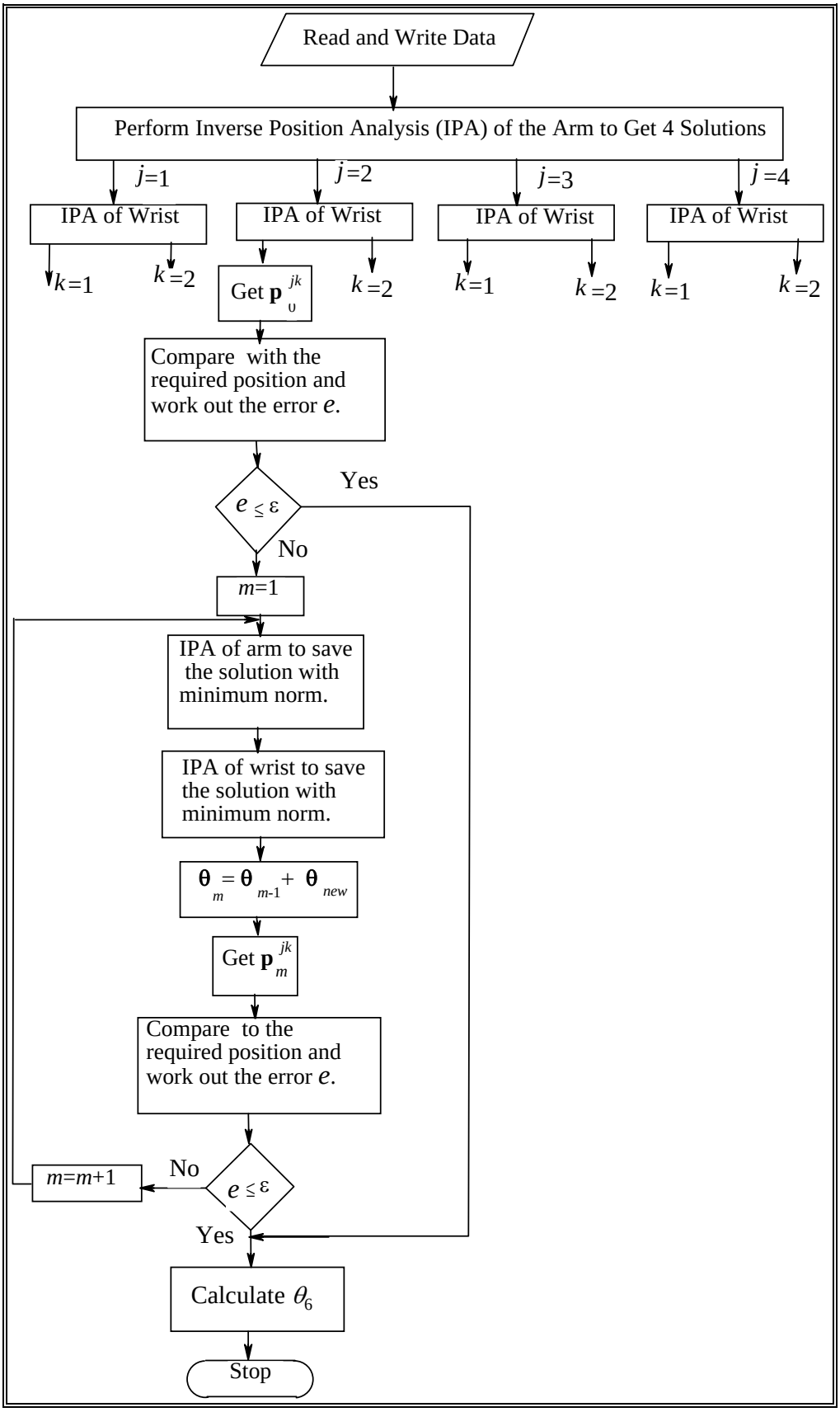

Figure (4): Inverse Position Analysis of Robots Using Elementary Motions.

correspond to this positioning task are therefore obtained using the models presented above and saved in four 3D-vectors, $\mathbf{v}_j$, where j=1,2,3 and 4.

At arm configuration number j, the wrist joints align the sixth joint-axis with its required final orientation, as described in section (5), and the two corresponding solutions are accordingly obtained and saved in a pair of 2D- vectors, $\mathbf{w}_{jk}$, where k may assume the values of 1 or 2. To this end, a set of eight joint-displacement solutions have been obtained. If the robot was of the spherical-wrist type these solutions should accurately represent the required joint-displacements and no iterations would be required.

Calibrated robots, however, are not likely to have their last three joint-axes intersecting at a common point (i.e. the spherical-wrist property was lost), the motions performed by the wrist joints will displace the point which was previously positioned by the arm to eight new locations, p_0^{jk}, corresponding to the wrist solutions obtained.

At location number jk, the instantaneous position vector, $\mathbf{p}_0^{jk}$, of the displaced point may be calculated, using a suitable direct kinematic procedure, and compared to the required position vector $\mathbf{p}_0^n$ where the net radial error, e_{jk}, is calculated as follows,

$$e_{jk} = \left\| \mathbf{p}_0^n - \mathbf{p}_0^{jk} \right\| \qquad (26)$$

If the calculated value for e_{jk} does not fall within an allowable error zone (e.g. 0. 01mm) the calculations proceed such that at iteration number m, the arm sets out from the most

updated configuration number jk(m-1) to position point p_{m-1}^{jk} in the required location. The four solutions obtained may be stored in four 3D-vectors whose norms are subsequently calculated and compared. Only the vector which corresponds to minimum norm, $\mathbf{v}_{jk}^{m}$, may be saved in the memory and the other solutions would be discarded. This vector is referred to here as the **arm elementary-motions vector** because it contains fractional quantities of elementary joint-displacements.

The two corresponding wrist solutions may then be obtained and stored in a pair of 2D-vectors whose norms will also be calculated and compared. The vector with minimum norm, $\mathbf{w}_{jk}^{m}$, is subsequently saved while the other vector may be disposed of. In the current context, $\mathbf{w}_{jk}^{m}$ is designated as the **wrist elementary-motions vector** because it contains small values of joint-displacements.

The new displaced location of the positioned point may then be calculated and compared with the required location as per equation (26). When the radial error is small enough, the final joint-displacement vector, $\mathbf{v}_{jk}^{n}$, of the arm group which corresponds to solution number jk may be calculated as follows,

$$\mathbf{v}_{jk}^{n} = \mathbf{v}_{j} + \sum_{m=1}^{M} \mathbf{v}_{jk}^{m} \qquad (27)$$

where M is the corresponding number of iterations.

The vector, $\mathbf{w}_{jk}^{n}$, which corresponds to the jk-solution of the wrist group may be expressed as follows,

$$\mathbf{w}_{jk}^{n} = \mathbf{w}_{jk} + \sum_{m=1}^{M} \mathbf{w}_{jk}^{m} \qquad (28)$$

Once the jk-solution for the first five joint-displacement has been obtained, the corresponding displacement of the last joint may simply be calculated.

The iterative technique proposed here utilises the physical kinematic behaviour of manipulator joints and therefore fast and singularity-proof convergence may be assured. The procedure is also suitable for use with parallel-computing facilities where each joint-displacement solution may be conveniently assigned to a different processor. The technique does not require any user-defined initial guesses introduced into the model.

8. Full-pose Alignment :

The work described in the previous sections is intended to locate the Z-axis of the sixth joint at its desired spatial position, p^{n}, and align it with the desired directional vector, $\mathbf{z}_{6}^{n}$. It is worth noting here that the tool (or end-effector) is pivoted to the sixth joint-axis and can only rotate about it. As such, once this axis is located in its desired position and direction in space, the tool needs to perform a single rotation about it to take its desired final pose. To calculate the required displacement, θ_6, of the sixth joint, the intermediate

directional vector, $\mathbf{x}_e^{int}$, of the tool X-axis (after having performed 5 rotations about the first 5 joint-axes) may be evaluated as follows,

$$\begin{bmatrix} \mathbf{x}_e^{int} \\ 0 \end{bmatrix} = {}_0\mathbf{T}^1 \, {}_1\mathbf{T}^2 \, {}_2\mathbf{T}^3 \, {}_3\mathbf{T}^4 \, {}_4\mathbf{T}^5 \, {}_5\mathbf{T}^6 \, {}_6\mathbf{T}^e \begin{bmatrix} \mathbf{x}_e^i \\ 0 \end{bmatrix} \tag{29}$$

where θ_6, in the above equation (29) is set equal to zero and $\mathbf{x}_e^i$ is given as, $(1 \quad 0 \quad 0)^T$. The transformation matrices, ${}_i\mathbf{T}^{i+1}$, are calculated as indicated in section (3); also the 3x3 rotational matrices can be used for this purpose.

The angular displacement, θ_6, can now be calculated by rotating $\mathbf{x}_e^{int}$ about $\mathbf{z}_6^n$ to coincide with the desired final direction of the X-axis of the tool, $\mathbf{x}_e^n$. This may be achieved by using the following equation,

$$\theta_6 = \mathbf{sign}(\mathbf{x}_e^{int} \times \mathbf{x}_e^n \circ \mathbf{z}_6^n) \tan^{-1} \left\{ \frac{\left| \mathbf{x}_e^{int} \times \mathbf{x}_e^n \right|}{\mathbf{x}_e^{int} \circ \mathbf{x}_e^n} \right\} \tag{30}$$

This final analysis is performed for every possible robot configuration and should ensure that a full-pose identification has now been performed for the end-effector.

9. Experimental Results :

The models described in the present paper have been implemented in an integrated approach developed for accurate kinematic control of robot manipulators. The ASEA IRB/L6 robot which is shown in Figure (5) was used for experimental verification of the results. At the selected zero-initial position, the ϕ-model parameters for both the calibrated and nominal robots are given in Table (1).

Table (1): ϕ-Model Parameters of the ASEA IRB/L6 Robot at the Zero-Initial-Position.

		Nominal Manipulator				Actual Manipulator			
frame	ϕ_i	a_i (m)	b_i (m)	α_i (deg)	β_i (deg)	a_i (m)	b_i (m)	α_i (deg)	β_i (deg)
1	90	0.0000	0.0000	90.0	-90.0	0.00232	0.0	90.0	-90.378
2	0.0	-0.6900	0.0000	90.0	-180.0	-0.6931	0.00487	89.828	-179.54
3	0.0	-0.6700	0.0000	90.0	-180.0	-0.6727	0.00162	90.4213	-179.99
4	0.0	0.0000	0.0000	90.0	-90.0	-0.0007	0.00297	89.8033	-89.921
5	0.0	0.0000	-0.2325	90.0	-90.0	-0.0039	-0.2331	89.4829	-90.137

The frame of the first joint-axis was taken as the base frame and the end-effector shared its Z-axis and origin with the sixth joint frame. This eliminates the need to include an arbitrarily-located frame in the model and therefore γ and h do not appear in the Table.

Position commands were then issued to the robot controller via the models described above and the end-effector position was measured, using theodoliltes, to evaluate the robot accuracy. The average value of this accuracy improved more than 33 fold (from 47 mm to 1.4 mm) since many sources of error (transducer deviations, gear train errors, geometric errors, …etc) were taken into account during the calibration procedure. The details of the calibration procedure may be sought in the work by Sultan and Wager (2001).

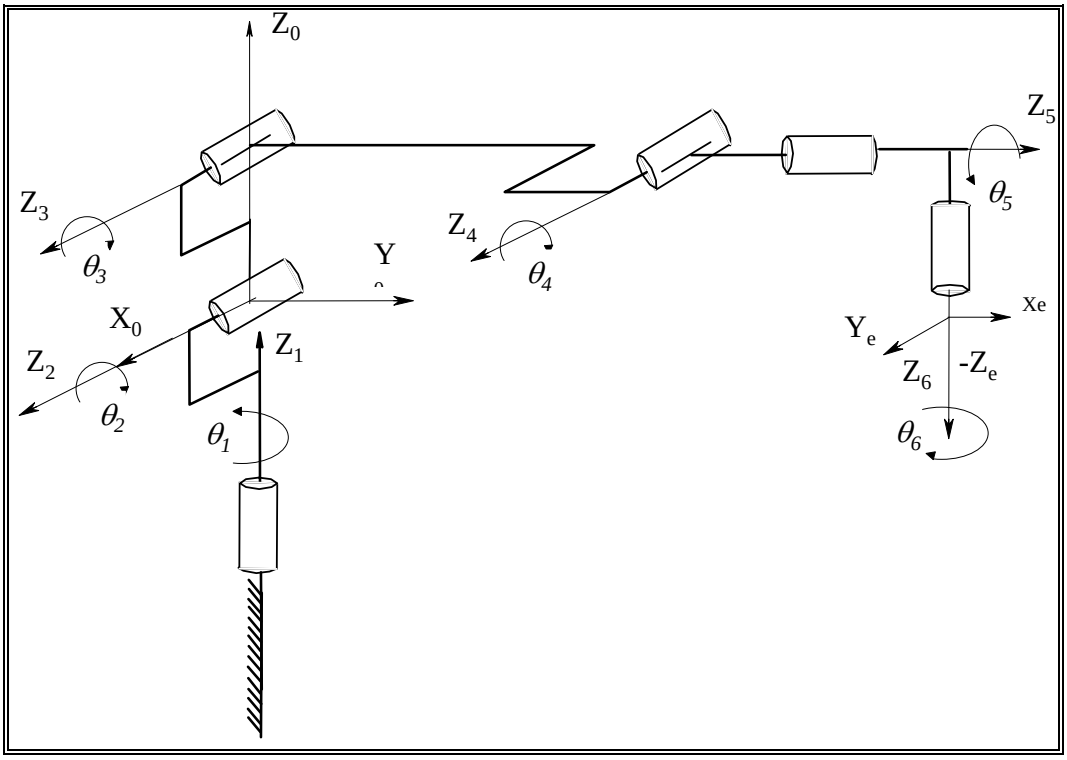

Figure (5): Schematic Diagram of the Robot Used for Experimental Verification.

One of the commanded positions was given, with respect to the Cartesian base coordinates, by the ${}_0\mathbf{T}^{en}$ matrix as follows,

$$ {}_0\mathbf{T}^{6n} = \begin{bmatrix} 0.328356 & 0.93926805 & 0.09976 & -197.7 \\ 0.914758 & -0.34253757 & 0.214198 & 636.1 \\ 0.235371 & 0.2092306 & -0.97168 & 852.0 \\ 0 & 0 & 0 & 1 \end{bmatrix} $$

where all lengths are in mm.

The initial hand pose, as measured by theodolites, is given as follows,

$$ {}_0\mathbf{T}^{6i}_{act} = \begin{bmatrix} -0.000764 & -0.999985 & -0.00538 & 1.49 \\ 0.999961 & -0.000181 & 0.0087983 & 903.32 \\ 0.008803 & 0.005383 & 0.999946 & 690.0 \\ 0 & 0 & 0 & 1 \end{bmatrix} $$

The results of the inverse position analysis which was performed on the robot are displayed in Table (2). The number of iterations which correspond to the physically-

attainable solution is equal to 6 and the allowable radial error (as per equation 26) used in the analysis was 0.007 mm. It should be noted here that the procedure produces no error in the orientation of the end-effector axis by the virtue of the iterative technique used as described in section 7. As such no convergence criterion is needed for orientation.

Table (2) Inverse Position Analysis Results for a Calibrated ASEA IRB/L6 Robot.

Sol. No.							
j	k	θ_1^{jk} deg	θ_2^{jk} deg.	θ_3^{jk} deg.	θ_4^{jk} deg.	θ_5^{jk} deg.	θ_6^{jk} deg.
1	1	17.35	18.13	-4.60	-3.70	-9.50	36.59
1	2	16.65	-23.57	46.43	167.39	-172.07	-144.37
2	1	16.53	-74.92	-174.82	-100.261	-8.30	35.48
2	2	16.02	-66.67	134.06	122.97	-172.73	-144.97
3	1	-162.06	74.183	-4.34	100.0	169.91	37.08
3	2	-162.72	65.70	47.161	-123.43	8.86	-143.84
4	1	-160.76	-18.572	-175.15	3.60	169.70	37.28
4	2	-162.27	23.28	-133.36	-167.22	8.77	-143.92

10. Conclusion:

An approach is proposed to obtain multiple inverse-position solutions for robotic structures. The procedure involved, which is suitable for both conventional and parallel computer applications, regards the manipulator as consisting of two open-ended mechanisms co-operating to place the end-effector at a desired spatial pose.

For calibrated robots, the procedure proposed adopts a simple iterative technique that does not require user-defined initial guesses and does not involve the use of the differential Jacobian-based models to eliminate the occurrence of singularity. Moreover, for spherical-wrist robots, the technique produces straight forward non-iterative solutions to the inverse position problem.

References:

1) Chiaverini, S., Siciliano, B. and Egeland, O., Review of the Damped Least-Squares Inverse kinematics with Experiments on an Industrial Robot Manipulator, IEEE Trans. Control Systems Technology, Vol. 2, No. 2, June 1994. pp. 123-134.

2) Coelho, P. H. G. and Nunes, L. F. A., Application of Kalman Filtering to Robot Manipulators, *Recent Trends in Robotics: Modelling, Control and Education*. Edited by Jamshidi, M., Luh, L. Y. S. and Shahinpoor, M. Elsevier Science Publishing Co., Inc., 1986, pp. 35-40.

3) Craig, John J., *Introduction to Robotics*, Addison-Wesley Publishing Company, 1986

4) Denavit, J. and Hartenberg, R. S., A Kinematic Notation for Low Pair Mechanisms Based on Matrices, ASME J. Appl. Mechanics, Vol. 22, June 1955, pp. 215-221.

5) Duffy, J. and Crane C., A Displacement Analysis of the General Spatial 7-Link, 7R Mechanism, Mech. Mach. Theory, Vol. 15, No. 3-A, 1980, pp. 153-169.

6) Goldenberg, A. A., Benhabib, B. and Fenton, R. G., A Complete Generalised Solution to the Inverse Kinematics of Robots, IEEE. Trans. on Robotics and Automation, Vol. RA-1, No. 1, March 1985, pp. 14-20.

7) Grudic, G. Z. and Lawrence, P. D., Iterative Inverse Kinematics with Manipulator Configuration Control, IEEE. Trans. on Robotics and Automation, Vol. 9, No. 4, August 1993, pp. 476-483.

8) Gu, Y.-L. and Luh, J. Y. S., Dual-Number Transformation and Its Application to Robotics, IEEE J Robotics and Automation, Vol. RA-3, No. 6, Dec. 1987, pp. 615-623.

9) Gupta, K., A Note on Position Analysis of Manipulators, Mech. Mach. Theory, Vol. 19, No. 1, 1984, pp. 5-8.

10) Hayati, S. and Roston, G., Inverse Kinematic Solution for Near-Simple Robots and Its Application to Robot Calibration, *Recent Trends in Robotics: Modelling, Control and Education*. Edited by, Jamshidi, M., Luh, L. Y. S. and Shahinpoor, M. Elsevier Science Publishing Co., Inc, 1986, 41-50.

11) Kohli, D. and Osvatic, M., Inverse Kinematics of General 6R and 5R,P Spatial Manipulators, ASME J. Mechanical Design, Vol. 115, Dec. 1993, pp. 922-930.

12) Lee, H.-Y. and Liang, C. G., A New Vector Theory for the Analysis of Spatial Mechanisms, Mech. Mach. Theory, Vol. 23, No. 13, 1988A, pp. 209-217.

13) Lee, H.-Y. and Liang, C. G., Displacement Analysis of the General Spatial 7-Link 7R Mechanism, Mech. Mach. Theory, Vol. 23, No. 13, 1988B, pp. 219-226.

14) Lee, H.-Y., Reinholtz, C. F., Inverse Kinematics of Serial-Chain Manipulators, ASME J. Mechanical Design, Vol. 118, Sept. 1996, pp. 396-404.

15) Mahalingam, S. and Sharan, A., The Nonlinear Displacement Analysis of Robotic Manipulators Using the Complex Optimisation Method, Mech. Mach. Theory, Vol. 22, No. 1, 1987, pp. 89-95.

16) Manocha, D. and Canny, J. F., Real Time Inverse Kinematics for General 6R Manipulators, Proc. IEEE Conf. on Robotics and Automation, Nice-France, May 1992, pp. 383-389.

17) Manseur, R. and Doty, K., A Complete Kinematic Analysis of Four-Revolute-Axis Robot Manipulators, Mech. Mach. Theory, Vol. 27, No. 5, 1992A, pp. 575-586.

18) Manseur, R. and Doty, K., A Robot Manipulator with 16 Real Inverse Kinematic Solution Sets, The Int. J. Robotics Research, Vol. 8, No. 5, October 1989, pp. 75-79.

19) Manseur, R. and Doty, K., Fast Algorithm for Inverse Kinematic Analysis of Robot Manipulators, The Int. J. Robotics Research, Vol. 7, No. 3, June 1988, pp. 52-63.

20) Manseur, R. and Doty, K., Fast Inverse Kinematics of Five-Revolute-Axis Robot Manipulators, Mech. Mach. Theory, Vol. 27, No. 5, 1992B, pp. 587-597.

21) Manseur, R. and Doty, K., Structural Kinematics of 6-Revolute-Axis Robot Manipulators, Mech. Mach. Theory, Vol. 31, No. 5, 1996, pp. 647-657.

22) Mooring, B. W., Roth, Z. S. and Driels, M. R., *Fundamentals of Manipulator Calibration*, John Wiley & Sons, New York, 1991.

23) Paul, R., *Robot Manipulators Mathematics, Programming and Control*, MIT Press, Cambridge, MA, 1981.

24) Phol, E. D. and Lipkin, H., Complex Robotic Inverse Kinematic Solutions, ASME J. Mechanical Design, Vol. 115, Sept. 1993, pp. 509-514.

25) Pieper, D. L. and Roth, B., The Kinematics of Manipulators Under Computer Control, Proc. 2nd Int. Congress on the Theory of Machines and Mechanisms, Vol. 2, Zakopane, Poland, 1969, pp. 159–168.

26) Poon, J. K. and Lawrence, P. D., Manipulator Inverse Kinematics Based on Joint Functions, Proc. IEEE Conf. on Robotics and Automation, Philadelphia, April 1988, pp. 669-674.

27) Pradeep, A. K., Yoder, P. J. and Mukundan, R., On the Use of Dual-Matrix Exponentials in Robotic Kinematic, The Int. J. Robotics Research, Vol. 8, No. 54, October 1989, pp. 57-66.

28) Raghavan, M. and Roth, B., Kinematic Analysis of the 6R Manipulator of General Geometry, Proceedings of the 5th Int. Symposium on Robotics Research, Tokyo, Aug. 28-31, 1989. pp. 263-269.

29) Smith, D. R. and Lipkin, H., Analysis of Fourth Order Manipulator Kinematics Using Conic Sections, Proc. IEEE Conf. on Robotics and Automation, Cincinnati 1990, pp. 274-278.

30) Sultan, I. A. and Trevelyan, J. P., Inverse Kinematic Analysis of Bent Robots, Proceedings of the Second International Conference On Automation, Robotics and Computer Vision, Singapore, Sept. 15-18, 1992.

31) Sultan. I. A. An Integrated Approach for Accurate Kinematic Control of Robot Manipulators, A PhD Thesis, The University of Western Australia, 1997.

32) Sultan, I. A. and Wager, J. G., User-Controlled Kinematic Modelling, Int. J. Advanced Robotics, Vol. 12, No. 6, pp 663-677, 1999.

33) Sultan, I. A. and Wager, J. G., A Technique for the Independent-axis Calibration of Robot Manipulators with Experimental Verification, Int. J. of Computer Integrated Manufacturing, Vol. 14, No. 5, 2001.

34) Tsai, L.-W. and Morgan, A. P., Solving the Kinematics of the Most General Six- and Five-Degree-of-Freedom Manipulators by Continuation Methods, ASME J. Mechanisms, Transmissions and Automation in Design, June 1985, Vol. 107, pp. 189-199.

35) Wang, K. and Bjorke, O., An Efficient Inverse Kinematic Solution with a Closed Form for Five-Degree-of-Freedom Robot Manipulators with a Non-Spherical Wrist, Annals of CIRP, Vol. 38, 1989, pp. 365-368.

36) Wang., L. T. and Chen, C. C., A Combined Optimisation Method for Solving the Inverse Kinematics Problem of Mechanical Manipulators, IEEE. Trans. on Robotics and Automation, Vol. 7, No. 4, August 1991, pp. 489-499.

37) Yang, A. T. and Freudenstein, F., Application of Dual-Numbers Quaternion Algebra to the Analysis of Spatial Mechanisms, ASME J. of Appl. Mechanics, June 1964, pp. 300-308.